

# Discovery and Identification of Contactlike Interactions in Fermion-pair Production at ILC

A. A. Pankov<sup>1</sup>, N. Paver<sup>2</sup> and A. V. Tsytinov<sup>1</sup>

1- ICTP Affiliated Centre, Pavel Sukhoi Technical University - Dept of Physics  
Gomel 246746 - Belarus

2- University of Trieste and INFN-Trieste Section - Dept of Theoretical Physics  
34100 Trieste - Italy

Non-standard scenarios described by effective contactlike interactions can be revealed only by searching for deviations of the measured observables from the Standard Model (SM) predictions. If deviations were indeed observed within the experimental uncertainty, the identification of their source among the different non-standard interactions should be needed. We here consider the example of the discrimination of gravity in compactified extra dimensions (ADD model) against the four-fermion contact interactions (CI). We present assessments of the identification reach on this scenario, that could be obtained from measurements of the differential cross sections for the fermionic processes  $e^+e^- \rightarrow \bar{f}f$ , with  $f = e, \mu, \tau, c, b$ , at the planned ILC.

## 1 Non-standard effective interactions

The non-standard contactlike local interactions we are going to consider are all characterized by corresponding large mass scales  $\Lambda_{\alpha\beta}$  and  $\Lambda_H$  to some inverse power that specifically depends on the dimension of the relevant effective local operators:

a) The compositeness inspired dim-6 four-fermion contact interactions (CI):

$$\mathcal{L}^{\text{CI}} = 4\pi \sum_{\alpha,\beta} \frac{\eta_{\alpha\beta}}{\Lambda_{\alpha\beta}^2} (\bar{e}_\alpha \gamma_\mu e_\alpha) (\bar{f}_\beta \gamma^\mu f_\beta), \quad \eta_{\alpha\beta} = \pm 1, 0, \quad (1)$$

with  $\alpha, \beta = \text{L, R}$  the helicities of the incoming and outgoing fermions [1]. Generally, this kind of models can describe exchanges between SM particles of very heavy  $W'$ ,  $Z'$ , leptoquarks, *etc.*

b) The ADD model of gravity in “large” compactified extra dimensions [2], that can be parameterized by the dim-8 contactlike interaction [3]:

$$\mathcal{L}^{\text{ADD}} = i \frac{4\lambda}{\Lambda_H^4} T^{\mu\nu} T_{\mu\nu}, \quad \lambda = \pm 1. \quad (2)$$

Here,  $T_{\mu\nu}$  is the energy-momentum of SM particles, and  $\Lambda_H$  essentially represents a cut-off on the exchange (in 4 dimensions) of a tower of Kaluza-Klein, spin-2, massive graviton excitations. For (sub)millimeter extra dimensions, the mass  $\Lambda_H$  scale may be expected to be of the TeV size.

In principle, in addition to the Planck mass  $M_D$  in  $4+n$  dimensions, such that  $M_{\text{PL}} = M_D^{1+n/2} R^{n/2}$  with  $R$  the compactification radius, there can exist one independent mass scale we denote generically as  $\Lambda$ , that represents the relative strength of tree *vs.* loop virtual

graviton exchanges. In the naive dimensional approximation (NDA), the relation of this extra scale to  $\Lambda_H$  in Eq. (2) is [4]:

$$\frac{1}{\Lambda_H^4} = \frac{\pi^{n/2}}{8\Gamma(n/2)} \frac{\Lambda_{\text{NDA}}^{n-2}}{M_D^{n+2}}. \quad (3)$$

Moreover, loops with virtual graviton exchanges can generate even 6-dimensional four-fermion interactions similar to the CI in Eq. (1). One example is the axial-axial operator:

$$\mathcal{L}_\Upsilon = \frac{1}{2} c_\Upsilon \left( \sum_f \bar{f} \gamma_\mu \gamma_5 f \right) \left( \sum_f \bar{f} \gamma^\mu \gamma_5 f \right), \quad (4)$$

with

$$c_\Upsilon = \frac{\pi^{n-2}}{16\Gamma^2(n/2)} \frac{\Lambda_{\text{NDA}}^{2+2n}}{M_D^{4+2n}}. \quad (5)$$

The current experimental lower bounds on the mass scales in Eqs. (1) and (2), that parametrize the strength of the corresponding contactlike interactions, can be summarized qualitatively as follows [5]:  $\Lambda_H > 1.3$  TeV;  $\Lambda_{\alpha\beta} > 10 - 15$  TeV [95% C.L.].

## 2 Discovery and identification of the ADD scenario

Clearly, constraints on  $\Lambda_{\alpha\beta}$  and  $\Lambda_H$  are determined by the deviations of the observables,  $\mathcal{O}$ , from the SM expectations. We choose as basic observables the longitudinally polarized differential cross sections,  $\mathcal{O} = d\sigma/d\cos\theta$ , for the fermionic processes  $e^+e^- \rightarrow ff$  at ILC ( $f$  is limited to  $e, \mu, \tau, c, b$ ). Obviously, the theoretical expressions of the cross sections including the novel physics (NP), to be compared to the data, are given by  $d\sigma \propto |\text{SM} + \text{NP}(\Lambda)|^2$ , where  $\Lambda$  generically denotes  $\Lambda_{\alpha\beta}$  or  $\Lambda_H$ . It has been strongly emphasized [6] that electron and positron beams polarization plays a crucial rôle in enhancing the sensitivity to the NP interactions and, indeed, this option is very seriously considered for the planned ILC.

The comparison between “theoretical” relative deviations,  $\Delta\mathcal{O}$ , and corresponding foreseen experimental relative uncertainties,  $\delta\mathcal{O}$ , can be performed by a simple  $\chi^2$  procedure combining the initial polarization configurations and the binning of the angular range for the measured reactions [7, 8]:

$$\Delta\mathcal{O} = \frac{\mathcal{O}(\text{SM} + \text{NP}) - \mathcal{O}(\text{SM})}{\mathcal{O}(\text{SM})}, \quad \chi^2(\mathcal{O}) = \sum_{\{P^-, P^+\}} \sum_{\text{bins}} \left( \frac{\Delta(\mathcal{O})^{\text{bin}}}{\delta\mathcal{O}^{\text{bin}}} \right)^2. \quad (6)$$

The  $\chi^2$  in Eq. (6) will be a function of the mass scale  $\Lambda$  relevant to the contactlike interaction under consideration. The expected *discovery* reach on an individual interaction, i.e., the maximum value of the corresponding mass scale  $\Lambda$  for which a deviation caused by the interaction itself could be observed, can be assessed by assuming a situation where no deviation is observed and imposing, for 95% C.L., the constraint  $\chi^2 \leq 3.84$ . Basically, this is the way the current limits above have been obtained.

In Table 1, we give examples of discovery reaches expected for an ILC with the “reference” parameters:  $\sqrt{s} = 0.5$  TeV; time-integrated luminosity  $\mathcal{L}_{\text{int}} = 500 \text{ fb}^{-1}$ , and electron and positron longitudinal polarizations  $|P^-| = 0.8$ ,  $|P^+| = 0.3$ . While these luminosity and

beams polarization seem guaranteed at the initial stage of ILC,  $\mathcal{L}_{\text{int}} = 1000 \text{ fb}^{-1}$  and  $|P^+|$  of the order of 0.6 may be considered, eventually, for later runs of the machine. To obtain the results in Table 1, binning of the angular range by  $\Delta \cos \theta = 0.2$  intervals has been used in (6), and the statistical uncertainties have been evaluated by the final fermions reconstruction efficiencies: 100% for electrons, 95% for  $\mu$  and  $\tau$ , 35% and 60% for  $c$  and  $b$  quarks, respectively. The dominant systematic uncertainties are found to originate from polarizations and luminosity, on which we have assumed the accuracies 0.1% and 0.5%, respectively. Earlier determinations, demonstrating the fundamental rôle of beams polarization for the discovery reaches on CI interactions, can be found, e.g., in Ref. [9]. The Table 1 shows the high sensitivity to  $\Lambda_{\alpha\beta}$  allowed by polarization, and that Bhabha scattering is the process most sensitive to  $\Lambda_H$ .

Model	Processes							
	$e^+e^- \rightarrow e^+e^-$		$e^+e^- \rightarrow l^+l^-$		$e^+e^- \rightarrow \bar{b}b$		$e^+e^- \rightarrow \bar{c}c$	
$\Lambda_H$	5.3;	5.5	3.7;	3.8	3.7;	4.0	3.7;	3.8
$\Lambda_{VV}^{ef}$	128.3;	136.7	136.4;	144.2	115.8;	137.4	128.3;	136.7
$\Lambda_{AA}^{ef}$	76.1;	90.3	122.4;	129.5	116.7;	139.5	116.9;	124.8
$\Lambda_{LL}^{ef}$	66.2;	82.7	81.9;	98.6	96.9;	105.7	84.1;	96.6
$\Lambda_{RR}^{ef}$	64.0;	81.5	78.4;	97.7	64.4;	98.0	71.5;	95.3
$\Lambda_{LR}^{ef}$	94.9;	100.1	74.1;	90.2	76.0;	95.9	54.5;	79.0
$\Lambda_{RL}^{ef}$	$\Lambda_{RL}^{ee} = \Lambda_{LR}^{ee}$		74.0;	90.6	70.9;	85.5	78.2;	86.5
$M_C$	20.5;	22.1	30.7;	32.5	9.7;	14.9	15.8;	17.3

Table 1: 95% C.L. discovery reaches (in TeV). Left and right entries in each column refer to the polarizations ( $|P^-|, |P^+|$ )=(0,0) and (0.8,0.3), respectively.

In principle, different interactions may cause similar deviations in (6), and one would need to identify, among the various contact interactions, the origin of the deviations, were they observed. In this regard, the *identification reach* on a given contact effective interaction can be defined as the maximum value of the characteristic mass scale  $\Lambda$  for which the considered interaction not only can cause observable deviations from the SM, but can also be discriminated as the source of the observed deviations against the other contact interactions for all values of *their* respective  $\Lambda$ s.

Earlier attempts to estimate the *identification reaches* on ADD and CI models in high energy  $e^+e^-$  reactions have been presented in Ref. [10]. We here continue with the  $\chi^2$  analysis outlined above [7, 8].

To make an illustrative example, we assume that the ADD model (2) is found to be consistent with observed deviations. To assess the level at which this scenario can be distinguished from each of the CI models of Eq. (1), one can consider the “distances” in the  $(\Lambda_H, \Lambda_{\alpha\beta})$  two-dimensional planes:

$$\tilde{\Delta}(\mathcal{O}) = \frac{\mathcal{O}(\text{CI}) - \mathcal{O}(\text{ADD})}{\mathcal{O}(\text{ADD})}, \quad \tilde{\chi}^2(\mathcal{O}) = \sum_{\{P^-, P^+\} \text{ bins}} \sum_{\text{bins}} \left( \frac{\tilde{\Delta}(\mathcal{O})^{\text{bin}}}{\tilde{\delta}\mathcal{O}^{\text{bin}}} \right)^2. \quad (7)$$

In Eq. (7), symbols are analogous to Eq. (6), except that the statistical component of the uncertainty  $\tilde{\delta}\mathcal{O}$  is now referred to the ADD model prediction. For each pair of  $\alpha, \beta$  subscripts, we can find *confusion* regions in the above mentioned planes, where models cannot be distinguished from each other at the 95% C.L., by imposing the conditions  $\tilde{\chi}^2(\Lambda_H, \Lambda_{\alpha\beta}) \leq 3.84$  for the pairs  $\alpha\beta = LL, RR, RL, LR$ . Each confusion region is enclosed by a contour that shows a minimum value of  $\Lambda_H, \Lambda_H^{(\alpha\beta)}$ , below which there is no confusion, namely, the “ $\alpha\beta$ ” CI model can be *excluded* as the source of the observed deviations for all values of  $\Lambda_{\alpha\beta}$ . Clearly, the smallest of the  $\Lambda_H^{(\alpha\beta)}$  determines the expected identification reach on the ADD model (2) [7]. This is exemplified in Figure 1, that refers to an ILC with  $\sqrt{s} = 0.5$  TeV,  $\mathcal{L}_{\text{int}} = 500 \text{ fb}^{-1}$  unpolarized (grey bars) and with polarized beams with  $|P^-| = 0.8, |P^+| = 0.3$  (black bars). The Figure indicates  $\Lambda_H^{\text{ID}} = 3.2$  TeV (3.5 TeV) as the expected identification reach on (2) for unpolarized (polarized) beams. The beams polarization, when combined as in (7), play a rôle in substantially restricting the confusion regions. This is even more evident by repeating the same procedure for the identification reaches on the CI couplings [7].

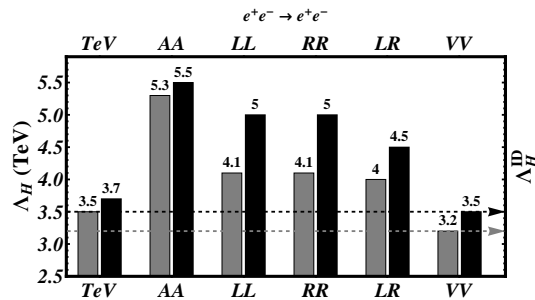


Figure 1: Exclusion and identification reaches on  $\Lambda_H$  at 95% C.L. obtained from Bhabha scattering.

### 3 Model-independent identification of the ADD scenario

In the previous section we compared *pairs* of individual contactlike interactions, (1) and (2). More generally, we can consider the possibility that, for a given final fermion flavour  $f$ , the CI interaction can be a linear combination of *all* the individual interactions in Eq. (1) with free, simultaneously non vanishing, independent coupling constants  $\eta_{\alpha\beta}/\Lambda_{\alpha\beta}^2$ . In this case, the corresponding identification reach on  $\Lambda_H$  would be defined as *model-independent*. The observables and their deviations in Ref. (7) now simultaneously depend on *all* mass scales  $\Lambda_{\alpha\beta}$  and  $\Lambda_H$  as  $\mathcal{O}(\text{CI}) = \mathcal{O}(\Lambda_{LL}, \Lambda_{RR}, \Lambda_{RL}, \Lambda_{LR})$ . The *confusion* region in the multi-parameter space  $(\Lambda_H, \Lambda_{\alpha\beta})$  with  $\alpha, \beta = L, R$ , where the general CI model can mimic the ADD model and therefore cannot be discriminated, is determined by the condition  $\tilde{\chi}^2 \leq \tilde{\chi}_{\text{crit}}^2$ . Here, for 95% C.L.,  $\tilde{\chi}_{\text{crit}}^2 = 9.49$  for the annihilation channels  $f = \mu, \tau, c, b$  and  $\tilde{\chi}_{\text{crit}}^2 = 7.82$  for Bhabha scattering ( $f = e$ ), where the LR and RL couplings are equal. As an illustration, we show in Figure 2 examples of the two-dimensional projections of the four-dimensional surface enclosing the 95% C.L. confusion region, onto the planes  $(\eta_{LL}/\Lambda_{LL}^2, \lambda/\Lambda_H^4)$  and  $(\eta_{LR}/\Lambda_{LR}^2, \lambda/\Lambda_H^4)$  for the cases of unpolarized beams (dashed curves) and both beams polarized with  $(|P^-|, |P^+|) = (0.8, 0.3)$  (solid lines). As one can see, the rôle of polarization in restricting the confusion region is dramatic.

As indicated by Figure 2, the contour of the confusion region identifies a minimal value of  $\Lambda_H$  for which the CI scenario can be excluded as the source of the deviations, and we take that value as the expected model-independent identification reach on the ADD scenario (2) [8]. The numerical results for such *model-independent identification reach*  $\Lambda_H^{\text{ID}}$  at the ILC, with parameters exposed in the caption, are shown in Table 2.

Using Eq. (3), we can turn the identification reach on  $\Lambda_H$  obtained above, into *allowed*

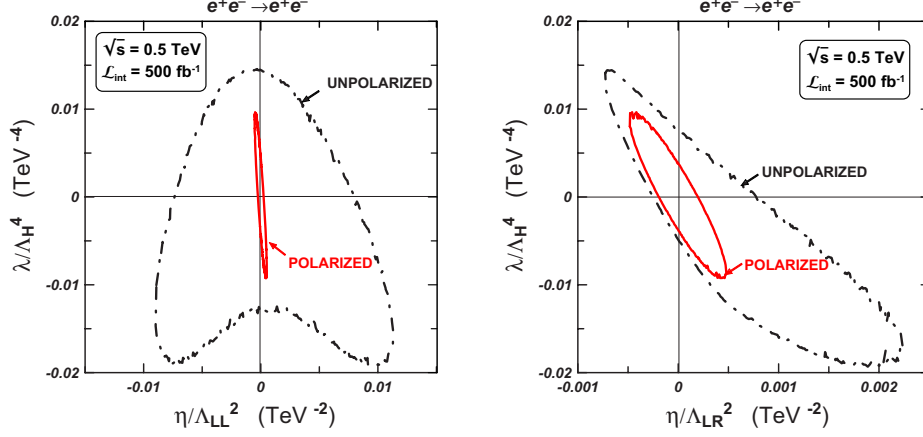


Figure 2: Two-dimensional projection of the 95% C.L. confusion region onto the planes  $(\eta_{LL}/\Lambda_{LL}^2, \lambda/\Lambda_H^4)$  and  $(\eta_{LR}/\Lambda_{LR}^2, \lambda/\Lambda_H^4)$  from Bhabha scattering .

$\Lambda_H$ (TeV)	Process	
	$e^+e^- \rightarrow e^+e^-$	combined $e^+e^- \rightarrow \bar{f}f$
$\mathcal{L}_{\text{int}} = 500 \text{ fb}^{-1}$	3.2	4.8
$\mathcal{L}_{\text{int}} = 1000 \text{ fb}^{-1}$	3.9	5.2

Table 2: 95% C.L. model-independent identification reach on  $\Lambda_H$  obtained from Bhabha scattering and combination of all final fermions ( $f = e, \mu, \tau, c, b$ ) at  $\sqrt{s} = 0.5$  TeV,  $\mathcal{L}_{\text{int}} = 500 \text{ fb}^{-1}$ ,  $(|P^-|, |P^+|) = (0.8, 0.3)$  and  $\mathcal{L}_{\text{int}} = 1000 \text{ fb}^{-1}$ ,  $(|P^-|, |P^+|) = (0.8, 0.6)$ , respectively.

and *excluded* regions in the two-dimensional  $(M_D, \Lambda_{\text{NDA}})$  plane at 95% C.L. An example, with  $n = 5$  and using the constraints expected from combined fermionic processes  $e, \mu, \tau, c, b$ , is shown in Figure 3 by the lines “ILC, G-exchange” for the two options:  $\mathcal{L}_{\text{int}} = 500 \text{ fb}^{-1}$ ,  $|P^-| = 0.8$ ,  $|P^+| = 0.3$  (thin solid curve) and  $\mathcal{L}_{\text{int}} = 1000 \text{ fb}^{-1}$ ,  $|P^-| = 0.8$ ,  $|P^+| = 0.6$  (thick solid curve).

Analogously, one can derive the identification reach on the coupling constant  $c_\Upsilon$  in Eq. (4), and then the corresponding 95% constraints in the  $(M_D, \Lambda_{\text{NDA}})$  plane *via* Eq. (5). The results, under the same conditions, are shown by the dashed lines “ILC, G-loops” in Figure 3. More details can be found in Ref. [8].

It should be interesting to compare our results on the  $M_D$  *v.s.*  $\Lambda_{\text{NDA}}$  allowed regions with the expectations from lepton-pair production  $p + p \rightarrow l^+l^- + X$  ( $l = e, \mu$ ) at the LHC (DY). We qualitatively assume that the same value of  $\Lambda$  enters into the different quark, antiquark and gluon subprocesses relevant to DY. Also, we attempt to assess the discrimination of deviations from the SM predictions caused by dimension-8 tree-level exchanges, Eqs. (2) and (3), from those due to the dimension-6 AA four-fermion interaction, Eqs. (4) and (5).

To this purpose, we utilize for the DY at the LHC the integrated angular “center-edge” asymmetry proposed in [11]. This observable has the property of being sensitive only to deviations from Eq. (2), but “transparent” to those from both Eq. (1) and Eq. (4). The identification reach obtained from DY at the LHC with  $\mathcal{L}_{\text{int}} = 100 \text{ fb}^{-1}$  (thick dot-dashed curve) is shown in Figure 3.

As Figure 3 shows, the limits on the tree-level graviton exchange parametrized by Eq. (2) and obtained from the LHC and ILC are complementary rather than competitive. Moreover, graviton-loop effects can dominate over tree-level exchange at larger  $M_D$ . In this regime, the identification of the effective operator  $c_\Upsilon$  in fermion pair production at ILC provide the most efficient probe of theories with extra dimensions. In this case, the ILC(0.5 TeV) for chosen values of the luminosity and beams polarization could be definitely superior to the LHC.

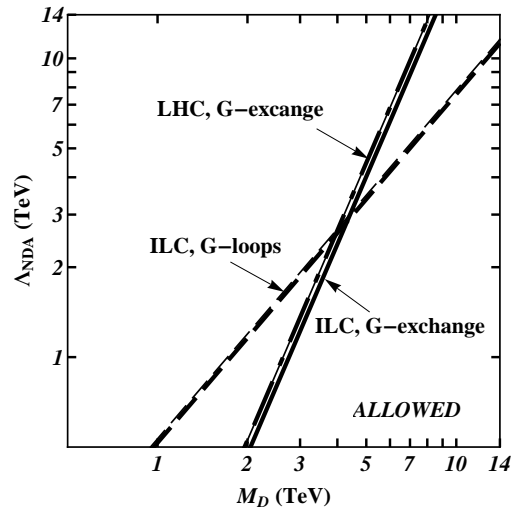


Figure 3: 95% C.L. identification reaches obtained at the polarized ILC(0.5 TeV) and LHC.

## 4 Acknowledgments

This work is partially supported by the ICTP through the OEA-Affiliated Centre-AC88.

## References

- [1] E. Eichten, K. D. Lane and M. E. Peskin, Phys. Rev. Lett. **50** 811 (1983); R. Rückl, Phys. Lett. **B129** 363 (1983).
- [2] N. Arkani-Hamed, S. Dimopoulos and G. R. Dvali, Phys. Lett. **B429** 263 (1998); I. Antoniadis, N. Arkani-Hamed, S. Dimopoulos and G. R. Dvali, Phys. Lett. **B436** 257 (1998).
- [3] J. L. Hewett, Phys. Rev. Lett. **82** 4765 (1999).
- [4] G. F. Giudice and A. Strumia, Nucl. Phys. **B663** 377 (2003); G. F. Giudice, T. Plehn and A. Strumia, Nucl. Phys. **B706** 455 (2005). [arXiv:hep-ph/0408320].
- [5] W. M. Yao *et al.* [Particle Data Group], J. Phys. G **33** 1 (2006).
- [6] G. Moortgat-Pick *et al.*, “The role of polarized positrons and electrons in revealing fundamental interactions at the linear collider”, arXiv:hep-ph/0507011 (2005).
- [7] A. A. Pankov, N. Paver and A. V. Tsytinov, Phys. Rev. **D73** 115005 (2006).
- [8] A. A. Pankov, A. V. Tsytinov and N. Paver, Phys. Rev. **D75** 095004 (2007).
- [9] S. Riemann, LC-TH-2001-007 (2001).
- [10] G. Pasztor and M. Perelstein, in *APS/DPF/DPB Summer Study on the Future of Particle Physics* (Snowmass 2001), edited by N. Graf, hep-ph/0111471; T. G. Rizzo, JHEP **0210** 013 (2002); P. Osland, A. A. Pankov and N. Paver, Phys. Rev. **D68** 015007 (2003); A. A. Pankov and N. Paver, Phys. Rev. **D72** 035012 (2005).
- [11] E. W. Dvergsnes, P. Osland, A. A. Pankov and N. Paver, Phys. Rev. **D69** 115001 (2004); E. W. Dvergsnes, P. Osland, A. A. Pankov and N. Paver, Int. J. Mod. Phys. **A20** 2232 (2005).